SIMULATING BIORESORBABLE LATTICE STRUCTURES TO ENABLE TIME-DEPENDENT STIFFNESS IN FRACTURE FIXATION DEVICES

Hawthorn, Barnaby (1);
Triantaphyllou, Andrew (2);
Khan, Farhan (2);
Dyson, Rosemary (3);
Thomas-Seale, Lauren E. J. (1)

1: School of Engineering, University of Birmingham;
2: The Manufacturing Technology Centre (MTC) Ltd, United Kingdom;
3: School of Mathematics, University of Birmingham, United Kingdom

ABSTRACT

Additive manufacture (AM) enables a greatly increased design freedom owing to its ability to manufacture otherwise difficult or impossible geometries. However, design creativity can often present itself as a barrier to realising the advantages that AM could offer. In this study the use of AM, bioresorbable materials and lattice design is considered as a method of satisfying contradicting design requirements during fracture healing. Often, immediately after a fracture high stiffness fixation is required; contradictingly during the remodelling phase high stiffness can inhibit bone healing. This study proposes the use of a bioresorbable body centred cubic (BCC) or face centred cubic (FCC) lattice structure to meet the need for tailored variation in implant stiffness over time. To reduce computational expense of lattice modelling a method is outlined, including the use of homogenisation. Results show homogenised representations perform within 5.2% and 1.4% for BCC and FCC unit cells respectively, with a 95% reduction in computational expense. Using resorption rates from the literature, time-dependent change in unit cell geometry was also modelled, showing the way in which a decrease in stiffness over time could be achieved.

Keywords: Additive Manufacturing, Biomedical design, Simulation, 4D Printing, Lattices

Contact:
Hawthorn, Barnaby
University of Birmingham
United Kingdom
BXH481@student.bham.ac.uk

Cite this article: Hawthorn, B., Triantaphyllou, A., Khan, F., Dyson, R., Thomas-Seale, L. E. J. (2023) 'Simulating Bioresorbable Lattice Structures to Enable Time-Dependent Stiffness in Fracture Fixation Devices', in *Proceedings of the International Conference on Engineering Design (ICED23),* Bordeaux, France, 24-28 July 2023. DOI:10.1017/pds.2023.318

1 INTRODUCTION

The design freedom of additive manufacturing (AM) offers an opportunity to create significant economic, societal and environmental impact, and tackle complex global challenges. However, over the last decade, design for AM (DfAM) has remained a barrier to the progression of this technology (RAENG, 2013). Creativity is often hailed as the solution to unleashing the untapped potential of AM, as such, this study presents a radical approach to meeting contradicting design constraints utilising AM.

The prioritisation of product requirements, during the design process is integral to various traditional methodologies (e.g. Analytic Hierarchy Process). Kanagalingam et al. (2019) demonstrate this problem, by mapping the biological process of fracture healing using the Theory of Inventive Problem Solving. The mechanical requirements of High Tibial Osteotomy (HTO) fixation are physically contradictory, including both stability and micromotion. Critically, the relative importance of these two requirements change over time; stability is required immediately after fracture but after approximately 6 weeks, interfragmentary motion governs the efficacy of healing. In this instance, changing the compliance of the fixation could offer enhanced healing, by enabling micromotion around the fracture site which changes over time.

Such a temporal variation of the performance of a component throughout its service could be promising concept for a number of applications beyond clinical challenges. Considering applications where it is difficult or even impossible for a human to activate the change required for a component's purpose, such as in deep sea instrumentation, deep space instrumentation, the adaptation of a component's function in response to some remote external stimulus could overcome this challenge. The literature denotes materials which respond to an external stimulus as SMART, and when integrated with AM, the technique is known as 4D printing. Predominately the stimuli for SMART materials are chemical, thermal or mechanical (Zhang, Demir and Gu, 2019). Rarely is time proposed as a method of controlling the function of a structure. Yet, the combination of biodegradable materials and AM could enable this.

This research will test the hypothesis that the compliance of a lattice structure, the design of which is enabled by AM, can be changed over time through the use of biodegradable materials. This research aims to simulate, in-silico, the change in the deformation of a biodegradable lattice with time. This research offers additional novelty by applying and validating homogenisation as a robust method of efficiently estimating the elastic deformation of FEMs of lattices.

2 BACKGROUND

2.1 Fracture fixation; stability and micromotion

Plate osteosynthesis has been used as a method of fracture fixation and healing as early as the late 19th century, since then it has progressed from conventional compression plates to modern locking plates with dynamisation techniques (Augat and von Rüden, 2018). It is well established understanding that overly rigid fixation inhibits the healing process through suppression of callus formation, leading to delayed union, nonunion, osteolysis and even fixation failure (Hak et al., 2010). Over rigid and over stiff fixation also leads to stress shielding, a phenomenon where the rate of bone resorption exceeds bone formation. This results in a lower density bone with poorer mechanical properties.

Micromotion at the site of fracture actually stimulates callus formation, leading to healing occurring more quickly and forming stronger bone – with early micromotion fostering increased bone density and stiffness (Jagodzinski and Christian, 2007). In the early phase of bone healing, as soft callus is being produced, interfragmentary motion utilising weight bearing or muscular contraction can stimulate the repair process (Augat, Hollensteiner and von Rüden, 2021). Thus the ideal requirements of fracture fixation, for example in the context of HTO, is a construct which is stiff enough to stabilise the fracture, which reduces with time to enable micromotion and thus improved healing (Kanagalingam et al., 2019).

2.2 Biodegradable and bioresorbable materials

To date, research into bioresorbable/biodegradable metals is far more limited than polymers. Polylactic acid (PLA), polyglycolic acid (PGA) and polycaprolactone (PCL) are amongst the most commonly used biocompatible polymers (Arif et al., 2019), with PLA also being the most commonly used bioresorbable

https://doi.org/10.1017/pds.2023.318 Published online by Cambridge University Press

polymer clinically today (da Silva et al., 2018; Thanigaiarasu, 2020). However, metals generally have a much longer resorption half-life when implanted, they are difficult to manufacture when compared to their polymer counterparts and metal related toxicity can be caused by corrosion (Hermawan, 2012; Prakasam et al., 2017). Bioresorbable metals include magnesium and magnesium alloys (Witte, 2010), zinc and zinc alloys (Kannan et al., 2017; Wen et al., 2018; Qin, Wen, Voshage, et al., 2019; Venezuela and Dargusch, 2019), and iron alloys (Hermawan, 2012). Conversely, the AM of non-degradable biocompatible materials, namely titanium and cobalt-chromium alloys, has seen success clinically and has been the subject of a wealth of research over recent years (Qin, Wen, Guo, et al., 2019). Whilst all of the aforementioned bioresorbable metals have been successfully manufactured using powder bed fusion (PBF) AM techniques, relatively the AM of these metals is still in its infancy. Zinc is considered to present the most promise for biodegradable applications as its degradation rate sits in between that of magnesium and iron counterparts (Mostaed et al., 2018).

2.3 Lattice simulation within FEA

During the design process, finite element analysis (FEA) tools are usually employed to model and analyse lattice unit cell configurations. Once the unit cell is designed, using FEA to model a full-scale lattice is computationally expensive. The computational time for these types of models is increased greatly due to the large number of degrees of freedom required when resolving each strut in the lattice structure (Alwattar and Mian, 2019). In the study by Koeppe et al. (2018) the simulation of a body centre cubic lattice with overall unit cell dimensions 5 x 5 x 5 mm^3, required 10 hours of computational time. To reduce this computational time, simplifications to lattice structures are often made.

Alternatively, homogenisation can be used to upscale the application of lattices structures in FEA (Tollenaere and Caillerie, 1998; Alwattar and Mian, 2019; Vlădulescu and Constantinescu, 2020). Homogenisation aims to determine the macroscopic mechanical properties of the lattice from the meso-scale properties of its unit cell (Arabnejad and Pasini, 2013; Omairey, Dunning and Sriramula, 2019). This circumvents having to model a full lattice structure geometry in any subsequent models, allowing the use of the overall macroscopic properties in a solid geometry instead, which reduces computational expense significantly. In work done by Alwattar and Mian (2019), FEA in conjunction with a neural network was used to homogenise the mechanical properties of a lattice unit cell, then predict mechanical properties of lattices with different unit cell configurations. Omairey, Dunning and Sriramula (2019) created an approach, integrated with FEA, which enables homogenisation based on any given unit cell, the goal being to simplify the modelling of lattice, cellular or composite components.

3 METHODS

3.1 Geometry

Unit cells chosen to investigate within this study were: face centred cubic (FCC), body centred cubic (BCC). Strut based unit cells were chosen due to their general suitability for additive manufacture (Benedetti et al., 2021) as well as their relative simplicity to model and mesh when compared to skeletal triply periodic minimal surface (TPMS) or sheet TPMS unit cells.

All unit cells were designed within Autodesk's Fusion 360 and then imported into Abaqus 2021 where they were partitioned. Each unit cell had overall dimensions of 5 × 5 × 5 mm^3 with an initial strut diameter of 1 mm and are depicted in Figure 1. It is important that the geometry of each unit cell is partitioned appropriately within Abaqus not only to ensure that a high quality mesh is generated, but also to ensure that nodes on opposing faces are directly mappable when creating periodic boundary conditions later on. This is achieved using the cell partition and face partition tools within Abaqus to partition the geometry as shown in Figure 1c and Figure 1d.

https://doi.org/10.1017/pds.2023.318 Published online by Cambridge University Press

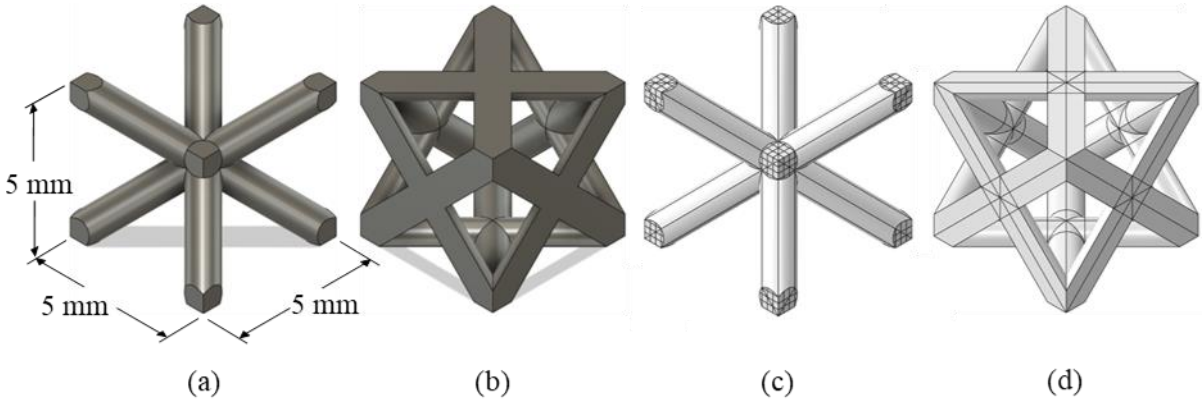

Figure 1 - Models of unit cells considered in this study: (a) body centred cubic (BCC), (b) face centred cubic (FCC), (c) partitioned BCC, (d) partitioned FCC

For validation, unit cell geometry was repeated to create a sample lattice spanning 5 × 5 × 5 unit cells in each direction, giving overall dimensions of 25 × 25 × 25 mm^3. The geometry of the homogenised equivalent model is therefore a solid cube of the same dimensions, these can be seen in Figure 2.

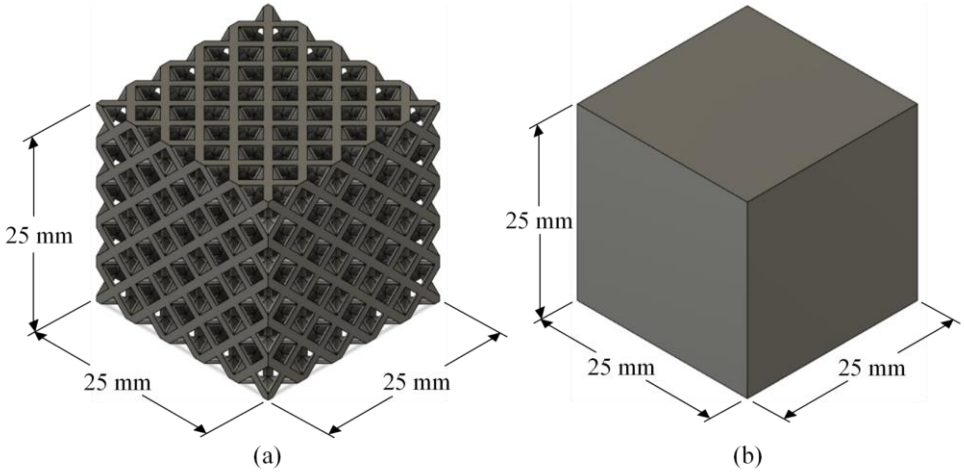

Figure 2 - (a) Standard 5 × 5 × 5 FCC unit cell lattice model geometry and (b) solid volume geometry of same dimensions used to compare performance of homogenised material

Standard lattice models were meshed with C3D10 tetrahedral elements in order to capture complex geometry, whereas homogenised equivalent representations were meshed with C3D8R brick elements as the geometry is simple. Mesh sensitivity analyses were performed to ensure spatial discretisation error is minimised, and a high quality mesh is ensured by monitoring important mesh quality metrics.

3.2 Materials

In this study two materials were applied to the finite element models. Firstly, material properties for pure zinc (Zn) manufactured using powder bed fusion laser beam (PBF-LB) were taken from literature by Wen et al. (2018). This material was chosen due to its aforementioned bioresorption properties being the ideal candidate for application in a lattice-based bioresorbable fracture fixation device. However, due to limitations with the availability of additively manufacturing such a material, it is unlikely that experimental validation of these lattice designs will be possible. In light of this limitation, readily available titanium alloy (Ti6Al4V) is also used in the model so that sample lattices can be additively manufactured and in-silico results can be more easily experimentally validated. Material properties of the two materials featured in the models are summarised below in Table 1.

Table 1 - Linear elastic material properties

Material	Elastic Modulus (GPa)	Poisson's Ratio	Density (kg/m^3)
Zn (PBF-LB)	23	0.25	7140
Ti6Al4V (PBF-LB)	132	0.34	4420

https://doi.org/10.1017/pds.2023.318 Published online by Cambridge University Press

In addition to standard lattice geometry, bioresorbable lattice geometries at time steps t_0, t_1 and t_2 were also created for simulation and use with zinc material properties; where t_0 is 0 weeks, t_1 is 26 weeks and t_2 is 52 weeks. Unit cells at t_0 have the same geometry shown in Figure 1, with additional unit cells created at t_1 and t_2 based on an in-vivo corrosion rate of 0.095 ± 0.009 mm/y from literature by Wang et al. (2019). Using Equation 1 the volumetric reduction of a unit cell over time can be calculated and taken into consideration in the design.

$$CR = {}^{\Delta V}/_{A \times t} \tag{1}$$

Where CR is the corrosion rate (mm/y), ΔV is volumetric reduction (mm^3), A is exposed surface area (mm^2) and t is time (years). This resorption rate results in an approximate 0.1 mm reduction in unit cell strut diameter over a 26 week period. An example of bioresorbable unit cells at time steps t_0, t_1 and t_2 can be seen below in Figure 3.

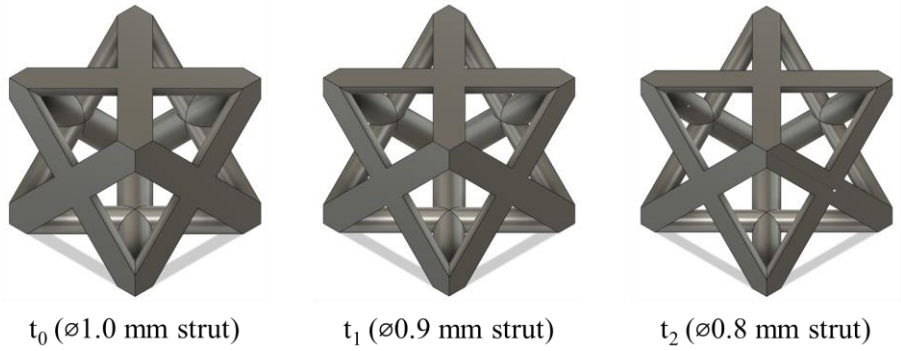

Figure 3 - Step-wise reduction in strut diameter due to bioresorption for FCC unit cell

3.3 Homogenisation

To complete the homogenisation of a unit cell, periodic boundary conditions must be implemented to capture accurate periodicity of the lattice and ensure that this is replicated in the homogenised material output. This can be achieved using the EasyPBC plugin (Omairey, Dunning and Sriramula, 2019) and Micromechanics plugin within Abaqus. All nodes on opposing faces are mapped to each other, with equation constraints added to restrict and link the relevant degrees of freedom. The unit cell will now behave as if it is part of a repeated array of unit cells, i.e. a lattice.

This method of homogenisation requires the imposition of uniform strains on the unit cell which in turn induces internal stresses within the unit cell which can be extracted from the Abaqus output file. With this information, equivalent macroscopic material properties of a unit cell can be calculated, as summarised in Figure 4 with the use of Equations 2 to 4. Micromechanics plugin for Abaqus creates required strain cases for homogenisation, post-processing the job data to output the macroscopic equivalent elastic material properties in the form of a full anisotropic material matrix. This macroscopic material representation can then be implemented into the homogenised model and its performance compared against a standard model.

$$E = \frac{Stress}{Axial\ Strain},\ E_{11} = \frac{\frac{\Sigma\ Front\ surface\ nodal\ forces_{in\ 1-Direction}}{Front\ surface\ area\ (H \times W)}}{\frac{\Delta L}{L}} \tag{2}$$

$$\nu = \frac{-Transverse\ Strain}{Axial\ Strain},\ \nu_{12} = \frac{\frac{\Delta H}{H}}{\frac{\Delta L}{L}},\ \nu_{13} = \frac{\frac{\Delta W}{W}}{\frac{\Delta L}{L}} \tag{3}$$

$$G = \frac{Shear\ Stress}{Tensors\ of\ Shear\ Strain},\ G_{12} = \frac{\frac{\Sigma\ Top\ surface\ nodal\ forces_{in\ 1-Direction}}{Top\ surface\ area\ (L \times W)}}{\frac{\Delta 1}{H} + \frac{\Delta 2}{L}} \tag{4}$$

https://doi.org/10.1017/pds.2023.318 Published online by Cambridge University Press

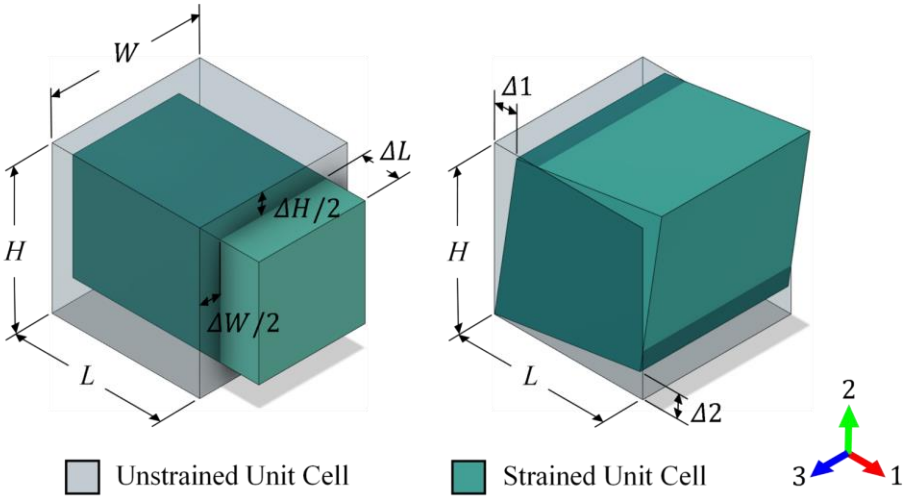

Figure 4 - Model subjected to displacements to estimate the macroscopic equivalent elastic modulus, Poisson's ratio and shear modulus (Omairey, Dunning and Sriramula, 2019)

3.4 Loads and boundary conditions

Samples are sandwiched between two rigid plates, the bottom of which is fixed at a reference point in the centre and the top constrained to move only in the Y-direction. Contact conditions were defined between contacting surfaces of the lattice or homogenised volume and the plates, with one corner of the lattice or homogenised volume being tied to the plate so that the sample cannot move from between the two plates. The concentrated loads are then applied in incremental loading steps to a reference point at the centre of the top plate such that the samples are compressed in the Y-direction. These loading conditions are displayed visually in Figure 5. The models are loaded in incremental loading steps such that the compressive force increases with each advancing loading step, summarised in Table 2. The models can be analysed at each step so that the deflection of the standard lattice can then be compared against the deflection of the solid volume incorporating the homogenised equivalent material properties.

Table 2 - A summary of the cumulative compressive loads applied to lattice models

	Load Step with Corresponding Compressive Force (N)					
Material	1	2	3	4	5	6
Zn	500	1000	2000	3000	4000	5000
Ti6Al4V	5000	10000	15000	20000	25000	30000

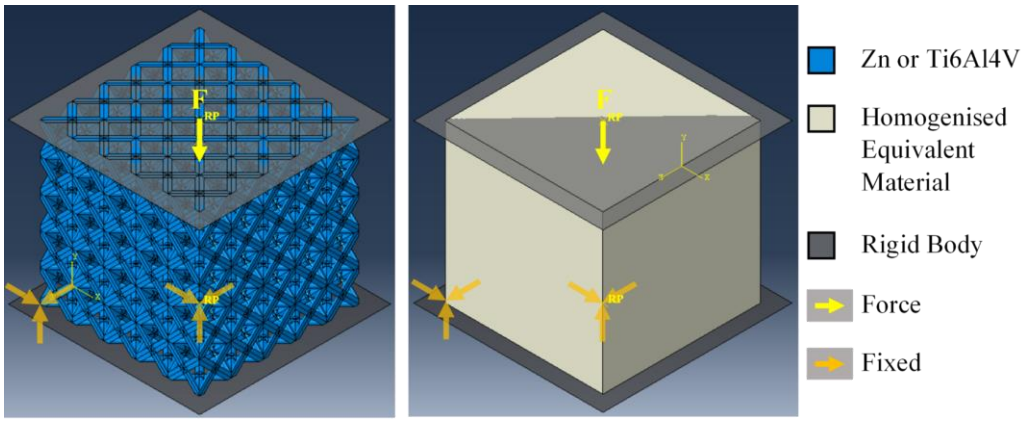

Figure 5 - Loading and boundary conditions for in-silico validation of homogenised simplification

https://doi.org/10.1017/pds.2023.318 Published online by Cambridge University Press

4 RESULTS AND DISCUSSION

4.1 Results

The average error when comparing the deflection of the standard FCC lattice sample to the homogenised equivalent model was 1.4%. Comparing the standard BCC lattice sample to the homogenised equivalent model the average error in deflection was 5.2%. These comparisons are shown graphically in Figure 6. When compared against experimental results from literature by Maskery et al. (2015), the homogenised equivalent elastic modulus of the Ti6Al4V BCC lattice determined using the method outlined above differs by less than 10%, giving confidence in the computational model.

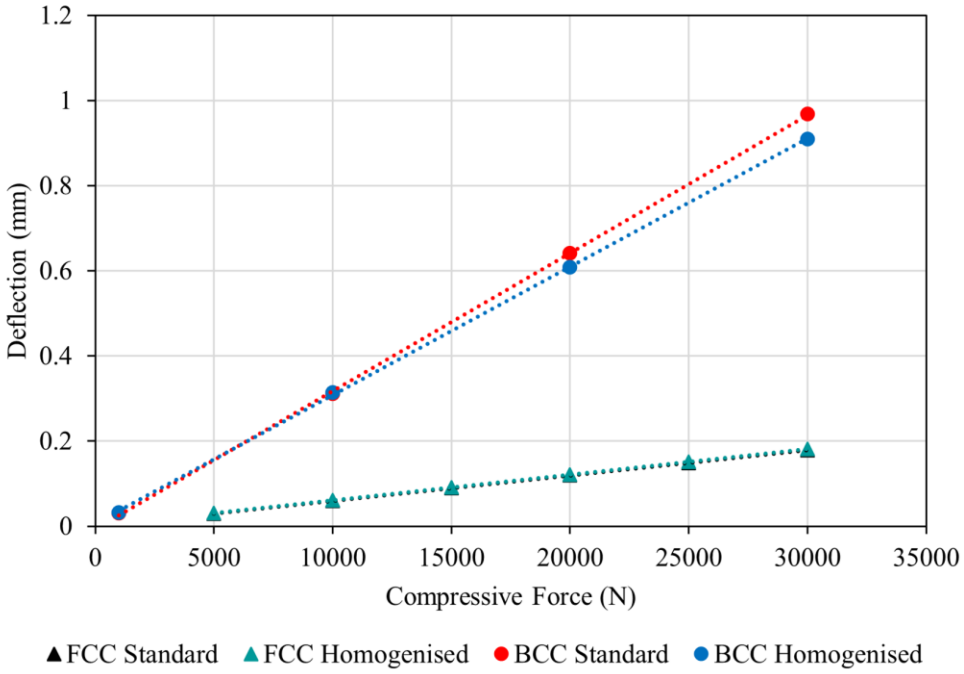

Figure 6 - Comparison of Ti6Al4V BCC and FCC standard lattice models with their homogenised equivalents

A reduction of approximately 95% for all metrics of computational expense was achieved through the use of a homogenised equivalent material instead of a full standard lattice model, this reduction in computational expense is summarised below in Table 3. In real-time terms, the standard lattice model took a total of 11 hours to run compared to the homogenised equivalent which took 30 minutes to run.

Table 3 - Summary of the reduction in computational expense across various metrics for standard 5 × 5 × 5 FCC model vs homogenised equivalent

	Standard Lattice		**Homogenised Equivalent**	**Percentage Reduction**
Input file (.inp)	235,142 KB	→	9375 KB	**96.0%**
Output file (.odb)	17,885,893 KB	→	497,749 KB	**97.2%**
Elements	1,222,143	→	74,088	**93.9%**
CPU Time	39721 sec	→	1989 sec	**95.0%**

For an FCC lattice which is able to bioresorb (i.e. manufactured from zinc), results comparing the deflection of a standard lattice model against a homogenised equivalent model at timepoints t_1, t_2, and t_3 are summarised in Figure 7. It can be seen that the homogenised model again performs similarly to the standard model, showing an average error of 1.4%. Additionally, as might be expected, the amount of deflection increases between time steps for the same amount of compressive force applied; i.e. the stiffness of the lattice decreases over time as the lattice bioresorbs.

https://doi.org/10.1017/pds.2023.318 Published online by Cambridge University Press

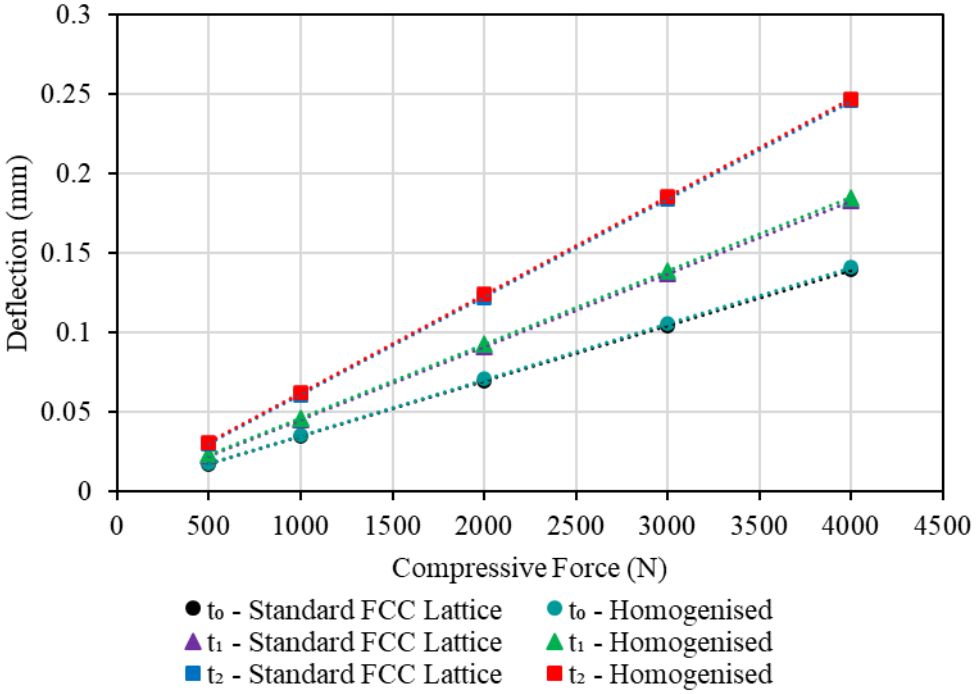

Figure 7 - Deflection of standard Zn FCC lattice vs homogenised at different time steps

4.2 Discussion

Figure 6 and Figure 7 show agreement between the standard lattice models and the homogenised equivalent models during compression for both FCC and BCC unit cell types respectively. In this study, simplifying lattice computation via homogenisation has created a very small amount of error relative to the large reduction in computational cost as summarised in Table 3. In the context of biomedical implant design and design of fracture fixation devices: if lattice structures were to be used within these devices, the simulation of many different types of unit cell would be required during the design process in order to arrive at a viable design. If modelled in their full complexity, these lattice-incorporating designs would be very computationally expensive to model. The results from this investigation show that homogenisation is a viable tool for simplifying this problem.

In this work bioresorption is modelled based on rates from literature (Wang et al., 2019) and implemented in a step-wise manner as shown in Figure 3. Homogenisation of these bioresorbable lattices was then investigated in the same way as with the standard titanium alloy lattices. Figure 7 illustrates the viability of simplifying the step-wise modelling of bioresorption in a lattice structure by using homogenisation, again showing minimal error along with a large reduction in computational expense. Additionally, as would be expected, Figure 7 shows a reduction in stiffness over time due to the resorption of material in the lattice structure. This demonstrates how this concept would be advantageous in not only designing for specific interfragmentary motion at the fracture site to stimulate callus formation and improve bone healing, but also in mitigating the earlier discussed problems of stress shielding and bone resorption which are generally caused due to over stiff fixation solutions.

There are still some improvements that could be made to the lattice modelling, in particular the geometric modelling of the lattice unit cells. In this work the unit cells are modelled with idealised struts, however in reality when manufactured the geometry does not perfectly represent that shown in Figure 1. This will not affect the error shown between in-silico comparisons of standard lattice models and homogenised equivalent models but could be a source of error and inaccuracy when comparing to experimental values of equivalent elastic modulus. Amongst other defects caused when additively manufactured, strut based lattices tend to show filleted geometries around where the struts meet due to the cumulative effect of residual heat from consecutive melted layers (Alghamdi et al., 2020). The addition of filleted edges on lattice unit cells can also provide other modelling advantages by removing common points where stress can concentrate resulting in a singularity (Lohmuller et al., 2018). Stress singularities can be sources of error within finite element models when not properly addressed (Song, Ooi and Natarajan, 2018) and having singularities around strut connections could introduce errors in the

https://doi.org/10.1017/pds.2023.318 Published online by Cambridge University Press

homogenisation process. To better anticipate defects such as this as well as mitigate any inaccuracies caused by stress concentration at unit cell corners during homogenisation, unit cell geometry could be modified to better represent manufactured outcomes such as that in Figure 8 below.

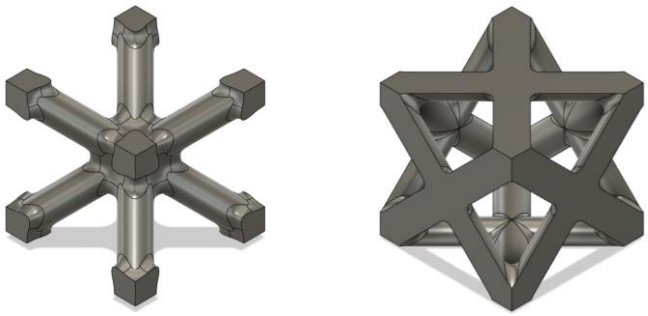

(a) (b)

Figure 8 - Unit cells incorporating 0.3 mm fillets at points where struts join, (a) BCC unit cell and (b) FCC unit cell

Principally the modelling of bioresorbable lattice structures within a fracture fixation device with the aim of tailoring its stiffness and stiffness modulation to the specific use case, requiring many iterations of different designs at many time steps, is suddenly a much more computationally viable problem.

5 CONCLUSIONS

In this work homogenised equivalent models are created to represent heterogenous lattice structures, accurately representing their more computationally expensive counterpart. Moreover, using this method to model bioresorbable lattices shows potential for tailoring lattice design to suit specific resorption and stiffness variation requirements. The study shows that:

- Homogenisation can reduce computational cost when simulating elastic behaviour of lattices by a factor of 20, whilst still maintaining low error of between 1.4% and 5.2% for FCC and BCC unit cells respectively.
- Lattice structures reduce in stiffness as their strut diameters decrease through resorption/degradation over time, allowing for increased deflection. There is potential to tailor this variation in stiffness through initial unit cell design.
- Modelling bioresorbable lattices using this method is more accessible than modelling a lattice geometry in its full complexity, bringing it within the bounds of industrial computation.

REFERENCES

Alghamdi, A. et al. (2020) 'Effect of additive manufactured lattice defects on mechanical properties: an automated method for the enhancement of lattice geometry', *The International Journal of Advanced Manufacturing Technology*, 108(3), pp. 957–971. Available at: https://doi.org/10.1007/s00170-020-05394-8.

Alwattar, T.A. and Mian, A. (2019) 'Development of an elastic material model for bcc lattice cell structures using finite element analysis and neural networks approaches', *Journal of Composites Science*, 3(2), p. 33. Available at: https://doi.org/10.3390/jcs3020033.

Arabnejad, S. and Pasini, D. (2013) 'Mechanical properties of lattice materials via asymptotic homogenization and comparison with alternative homogenization methods', *International Journal of Mechanical Sciences*, 77, pp. 249–262. Available at: https://doi.org/10.1016/j.ijmecsci.2013.10.003.

Arif, U. et al. (2019) 'Biocompatible Polymers and their Potential Biomedical Applications: A Review', *Current Pharmaceutical Design*, 25(34), pp. 3608–3619. Available at: https://doi.org/10.2174/1381612825999191011105148.

Augat, P., Hollensteiner, M. and von Rüden, C. (2021) 'The role of mechanical stimulation in the enhancement of bone healing', *Injury*, 52, pp. S78–S83. Available at: https://doi.org/10.1016/j.injury.2020.10.009.

Augat, P. and von Rüden, C. (2018) 'Evolution of fracture treatment with bone plates', *Injury*, 49, pp. S2–S7. Available at: https://doi.org/10.1016/S0020-1383(18)30294-8.

Benedetti, M. et al. (2021) 'Architected cellular materials: A review on their mechanical properties towards fatigue-tolerant design and fabrication', *Materials Science and Engineering: R: Reports*, 144, p. 100606. Available at: https://doi.org/10.1016/j.mser.2021.100606.

https://doi.org/10.1017/pds.2023.318 Published online by Cambridge University Press

Hak, D.J. et al. (2010) 'The Influence of Fracture Fixation Biomechanics on Fracture Healing', *Orthopedics*, 33(10).
Hermawan, H. (2012) 'Biodegradable Metals: State of the Art', in. Springer, Berlin, Heidelberg, pp. 13–22. Available at: https://doi.org/10.1007/978-3-642-31170-3_2.
Jagodzinski, M. and Christian, K. (2007) 'Effect of mechanical stability on fracture healing — an update', *Injury*, 38(1), pp. S3–S10.
Kanagalingam, S. et al. (2019) 'Design Principles to Increase the Patient Specificity of High Tibial Osteotomy Fixation Devices'. Available at: https://doi.org/10.1017/dsi.2019.96.
Kannan, M.B. et al. (2017) 'Biocompatibility and biodegradation studies of a commercial zinc alloy for temporary mini-implant applications', *Scientific Reports*, 7(1). Available at: https://doi.org/10.1038/s41598-017-15873-w.
Koeppe, A. et al. (2018) 'Efficient numerical modeling of 3D-printed lattice-cell structures using neural networks', *Manufacturing Letters*, 15, pp. 147–150. Available at: https://doi.org/10.1016/j.mfglet.2018.01.002.
Lohmuller, P. et al. (2018) 'Stress Concentration and Mechanical Strength of Cubic Lattice Architectures', *Materials*, 11(7), p. 1146. Available at: https://doi.org/10.3390/ma11071146.
Maskery, I. et al. (2015) 'Mechanical Properties of Ti-6Al-4V Selectively Laser Melted Parts with Body-Centred-Cubic Lattices of Varying cell size', *Experimental Mechanics*, 55(7), pp. 1261–1272. Available at: https://doi.org/10.1007/s11340-015-0021-5.
Mostaed, E. et al. (2018) 'Zinc-based alloys for degradable vascular stent applications', Acta Biomaterialia. Acta Materialia Inc. Available at: https://doi.org/10.1016/j.actbio.2018.03.005.
Omairey, S.L., Dunning, P.D. and Sriramula, S. (2019) 'Development of an ABAQUS plugin tool for periodic RVE homogenisation', *Engineering with Computers*, 35(2), pp. 567–577. Available at: https://doi.org/10.1007/s00366-018-0616-4.
Prakasam, M. et al. (2017) 'Biodegradable materials and metallic implants-A review', *Journal of Functional Biomaterials. MDPI AG*. Available at: https://doi.org/10.3390/jfb8040044.
Qin, Y., Wen, P., Guo, H., et al. (2019) 'Additive manufacturing of biodegradable metals: Current research status and future perspectives', *Acta Biomaterialia*. Acta Materialia Inc. Available at: https://doi.org/10.1016/j.actbio.2019.04.046.
Qin, Y., Wen, P., Voshage, M., et al. (2019) 'Additive manufacturing of biodegradable Zn-xWE43 porous scaffolds: Formation quality, microstructure and mechanical properties', *Materials and Design*, 181, p. 107937. Available at: https://doi.org/10.1016/j.matdes.2019.107937.
RAENG (2013) 'Additive manufacturing: opportunities and constraints'. *Royal Academy of Engineering*. Available at: https://raeng.org.uk/media/ak3htcyo/additive_manufacturing.pdf (Accessed: 18 November 2022).
da Silva, D. et al. (2018) 'Biocompatibility, biodegradation and excretion of polylactic acid (PLA) in medical implants and theranostic systems', *Chemical Engineering Journal*, 340, pp. 9–14. Available at: https://doi.org/10.1016/j.cej.2018.01.010.
Song, C., Ooi, E.T. and Natarajan, S. (2018) 'A review of the scaled boundary finite element method for two-dimensional linear elastic fracture mechanics', *Engineering Fracture Mechanics*, 187, pp. 45–73. Available at: https://doi.org/10.1016/j.engfracmech.2017.10.016.
Thanigaiarasu, P. (2020) 'Biomimetics in the design of medical devices', in *Trends in Development of Medical Devices*. Elsevier Inc., pp. 35–41. Available at: https://doi.org/10.1016/B978-0-12-820960-8.00003-4.
Tollenaere, H. and Caillerie, D. (1998) 'Continuous modeling of lattice structures by homogenization', Advances in Engineering Software, 29(7–9), pp. 699–705. Available at: https://doi.org/10.1016/S0965-9978(98)00034-9.
Venezuela, J. and Dargusch, M.S. (2019) 'The influence of alloying and fabrication techniques on the mechanical properties, biodegradability and biocompatibility of zinc: A comprehensive review', *Acta Biomaterialia*. Acta Materialia Inc. Available at: https://doi.org/10.1016/j.actbio.2019.01.035.
Vlădulescu, F. and Constantinescu, D.M. (2020) 'Lattice structure optimization and homogenization through finite element analyses', *Proceedings of the Institution of Mechanical Engineers*, Part L: Journal of Materials: Design and Applications, 234(12), pp. 1490–1502. Available at: https://doi.org/10.1177/1464420720945744.
Wang, X. et al. (2019) 'In vivo study of the efficacy, biosafety, and degradation of a zinc alloy osteosynthesis system', *Acta Biomaterialia*, 92, pp. 351–361. Available at: https://doi.org/10.1016/j.actbio.2019.05.001.
Wen, P. et al. (2018) 'Laser additive manufacturing of Zn metal parts for biodegradable applications: Processing, formation quality and mechanical properties', *Materials and Design*, 155, pp. 36–45. Available at: https://doi.org/10.1016/j.matdes.2018.05.057.
Witte, F. (2010) 'The history of biodegradable magnesium implants: A review', *Acta Biomaterialia*. Elsevier. Available at: https://doi.org/10.1016/j.actbio.2010.02.028.
Zhang, Z., Demir, K.G. and Gu, G.X. (2019) 'Developments in 4D-printing: a review on current smart materials, technologies, and applications', *International Journal of Smart and Nano Materials*, 10(3), pp. 205–224. Available at: https://doi.org/10.1080/19475411.2019.1591541.